PAMM · Proc. Appl. Math. Mech. **4**, 23–26 (2004) / **DOI** 10.1002/pamm.200410006

On the Optimization of Non-Negative Density Solutions of Stationary Fokker-Planck Equations

Walter V. Wedig *

Universität Karlsruhe, D-76128 Karlsruhe, Germany

Classical solution methods of Fokker-Planck equations (see e.g. [1],[2],[3]) lead to negative densities at least in the tales where the density solutions strongly approach zero. To avoid these inconsistencies the paper proposes to apply central differences schemes in combination with large-scaled quadratic optimization programming [4].

1 Introduction to the problem

Stochastic dynamical systems are investigated in the time domain by direct path-wise integration along the process trajectories or indirect in the space domain by solving associated Fokker-Planck equations to determine relative frequencies or probabilities of the processes. To test details of integration, consider the example of a linear scalar system described by the Itô equation

$$dX_t = -\omega_g X_t dt + \sigma dW_t, \qquad E(dW_t^2) = dt. \tag{1}$$

Herein, ω_g is a limiting frequency of the low-pass process X_t and σ is the intensity parameter of its excitation by the increments dW_t of the Wiener process W_t. It is suitable to introduce dimensionless time and state by

$$X_t = \bar{X}_t \sqrt{E(X_t^2)}, \qquad \text{with} \quad E(X_t^2) = \sigma^2/(2\omega_g), \tag{2}$$

$$d\tau = \omega_g dt, \qquad dW_\tau = \sqrt{\omega_g}\, dW_t. \tag{3}$$

The introduction of both dimensionless quantities into the system equation (1) leads to the parameter free equation

$$d\bar{X}_\tau = -\bar{X}_\tau d\tau + \sqrt{2} dW_\tau, \qquad E(dW_\tau^2) = d\tau. \tag{4}$$

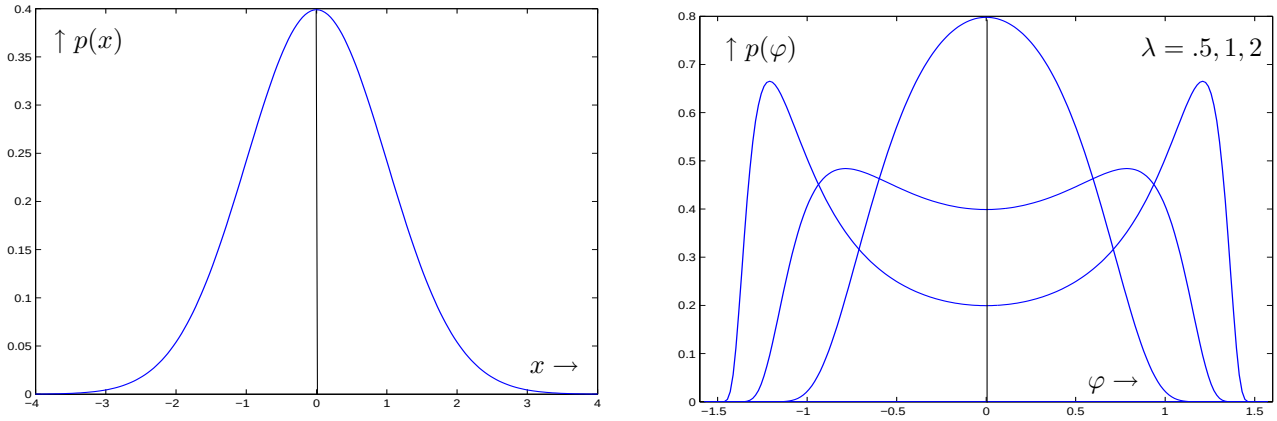

Fig. 1 a) Normalized Gaussian density. b) Density transformed by $\varphi = \arctan \lambda x$.

It possesses the Fokker-Planck equation (5) which is easily integrated under the stationarity condition $\partial p/\partial \tau = 0$.

$$\frac{\partial p(x,\tau)}{\partial \tau} = -\frac{\partial}{\partial x}[x p(x,\tau)] - \frac{1}{2}\frac{\partial^2}{\partial x^2}[2p(x,\tau)], \tag{5}$$

$$p(x) = \frac{1}{\sqrt{2\pi}} \exp(-\frac{1}{2}x^2), \qquad \text{for} \quad |x| \le \infty. \tag{6}$$

Herein, $p(x)$ is the well-known stationary density solution of the Fokker-Planck equation (5). The left picture in figure 1 shows the numerical evaluation of $p(x)$ in the range $|x| \le 4$.

* Corresponding author: e-mail: wedig@itm.uni-karlsruhe.de, Phone: 0049 721 608 2658, Fax: 0049 721 608 6070

2 Transformation to finite solution ranges

Under the stationarity condition $\partial p/\partial\tau = 0$ the Fokker-Planck equation (5) leads to an ordinary differential equation which has to be solved under the two boundary conditions $p(x = 0) = C$ and $p(x = \pm\infty) = 0$. Both are necessary to fulfill the normalization condition that the integration of $p(x)$ over the entire range $|x| \leq \infty$ is one. Because of the homogeneity of the Fokker-Planck equation the constant C represents a simple factorization and can be chosen to one without any loss of generality. Vanishing density boundaries on $x = \pm\infty$ are necessary to satisfy the radiation conditions that the solution process remains inside the range $|x| \leq \infty$. To investigate these singular boundaries numerically, the transformation $\phi = \arctan \lambda x$ is introduced with $0 < \lambda < \infty$. Provided that λ is a free parameter with finite values, the $arctan$-transformation reduces the singular density range $|x| \leq \infty$ to the finite one $|\varphi| \leq \pi/2$ leading to the transformed density distribution

$$p(\varphi) = \frac{1}{\lambda\sqrt{2\pi}\cos^2\varphi}\exp(-\frac{\tan^2\varphi}{2\lambda^2}), \qquad \text{for} \quad |\varphi| \leq \pi/2, \tag{7}$$

It is shown in the right side of figure 1 for the three parameter values $\lambda = .5, 1$ and $\lambda = 2$. Associated to the transformed density, above, there is a transformed Itô equation of the form

$$d\Phi_\tau = -(1 + 2\lambda^2\cos^2\Phi_\tau)\sin\Phi_\tau\cos\Phi_\tau d\tau + \sqrt{2}\lambda\cos^2\Phi_\tau dW_\tau, \tag{8}$$

which is derived applying Itô's calculus [5] to the angle process $\Phi_\tau = \arctan\lambda\bar{X}_\tau$. The transformed stochastic differential equation (8) leads to the Fokker-Planck equation

$$\frac{\partial}{\partial\varphi}[(\frac{1}{\lambda^2} + 2\cos^2\varphi)\sin\varphi\cos\varphi p(\varphi)] + \frac{\partial^2}{\partial\varphi^2}[\cos^4\varphi p(\varphi)] = 0, \tag{9}$$

when the stationary density solution is of interest only.

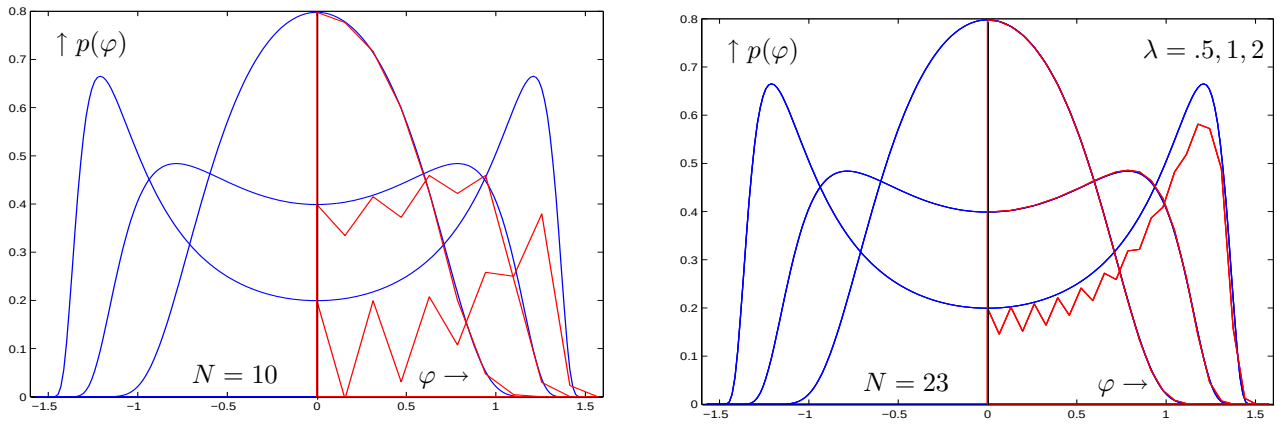

Fig. 2 Discrete and exact solutions of the Fokker-Planck equation (10) for the density parameters $\lambda = .5, 1, 2$.

3 Application of central differences schemes

The stationary Fokker-Planck equation (9) of the transformed system can once be integrated leading to the first order form

$$(\frac{1}{\lambda^2} - 2\cos^2\varphi)\sin\varphi\cos\varphi\, p(\varphi) + \cos^4\varphi\frac{\partial}{\partial\varphi}[p(\varphi)] = C. \tag{10}$$

Herein, C is a constant of integration which is vanishing when symmetry respectively radiation conditions have to be satisfied. Subsequently, one cosine function in (10) can be cancelled out. Applying the central difference scheme by $dp/d\varphi \approx (p_{n+1} - p_{n-1})/(2\Delta\varphi)$ with the step size $\Delta\varphi = \pi/(2N)$, the discrete form of the Fokker-Planck equation (10) is derived to

$$a_n p_n + c_n^3 p_{n-1} - c_n^3 p_{n+1} = 0, \qquad c_n = \cos n\Delta\varphi, \tag{11}$$

$$a_n = (2c_n^2 - \frac{1}{\lambda^2})2s_n\Delta\varphi, \qquad s_n = \sin n\Delta\varphi. \tag{12}$$

It is valid for all $n = 1, 2, \ldots, N-1$. Provided that the density solution is symmetric, the following boundary conditions are to be satisfied:

$$p_0 = 1, \text{ (Normalization)}, \qquad p_N = 0. \text{ (Radiation Condition)} \tag{13}$$

Obviously, this discrete formulation leads to $N-1$ inhomogeneous equations to be evaluated for given $\lambda-$parameter and step size $\Delta\varphi$. Figure 2 shows evaluations for the parameters $\lambda = .5, 1, 2$ and for $N = 10$ steps on the left picture and $N = 23$ on the right-hand side. Correspondingly, the discrete solutions are stable showing good coincidences with the exact solutions for low parameter values λ and small step sizes $\Delta\varphi$. For high parameters λ, the step number N has to be sufficiently increased to obtain a smooth density close to the exact solution.

4 Application of central differences schemes

Performing all differentiations with respect to φ, the second order Fokker-Planck equation (9) takes the form

$$c^4\frac{d^2p}{d\varphi^2} - 6sc^3\frac{dp}{d\varphi} - 2c^2(c^2-3s^2)p + \frac{1}{\lambda^2}[sc\frac{dp}{d\varphi} + (c^2-s^2)p] = 0, \qquad |\varphi| \le \pi/2. \tag{14}$$

Herein, c and s are abbreviations for $c = \cos\varphi$ and $s = \sin\varphi$, respectively. Applying the central differences scheme with the step size $\Delta\varphi = \pi/(2N)$ leads to the discrete version of (14)

$$\alpha_n p_n + \beta_n p_{n+1} + \gamma_n p_{n-1} = 0, \qquad\qquad n = 1, 2, \ldots, N-1. \tag{15}$$

This recursion formula possesses the coefficients α_n, β_n and γ_n calculated to

$$\alpha_n = 2c_n^4 + 2c_n^2(c_n^2 - 3s_n^3)\Delta\varphi^2 - (c_n^2 - s_n^2)\Delta\varphi^2/\lambda^2, \qquad s_n = \sin n\Delta\varphi, \tag{16}$$

$$\beta_n(\gamma_n) = -c_n^4 \pm 3c_n^3 s_n\Delta\varphi \mp c_n s_n\Delta\varphi/(2\lambda^2), \qquad c_n = \cos n\Delta\varphi. \tag{17}$$

Figure 3 shows evaluations of (15) together with the exact solutions (7) for $N = 10$ and $\lambda = .5$ in the left picture, respectively for $N = 40$ and $\lambda = 2$ in the right one. The left sides in both pictures are calculated under the same boundary conditions $p_0 = 1$ and $p_N = 0$, as previously applied. The right sides in both pictures show solutions which satisfy $p_0 = 1$ and $p_1 = p_{-1}$. Obviously, these boundary conditions are less optimal. The associated solutions diverge strongly on the right-hand side at the boundary $n = N$ and $\varphi = \pi/2$, respectively.

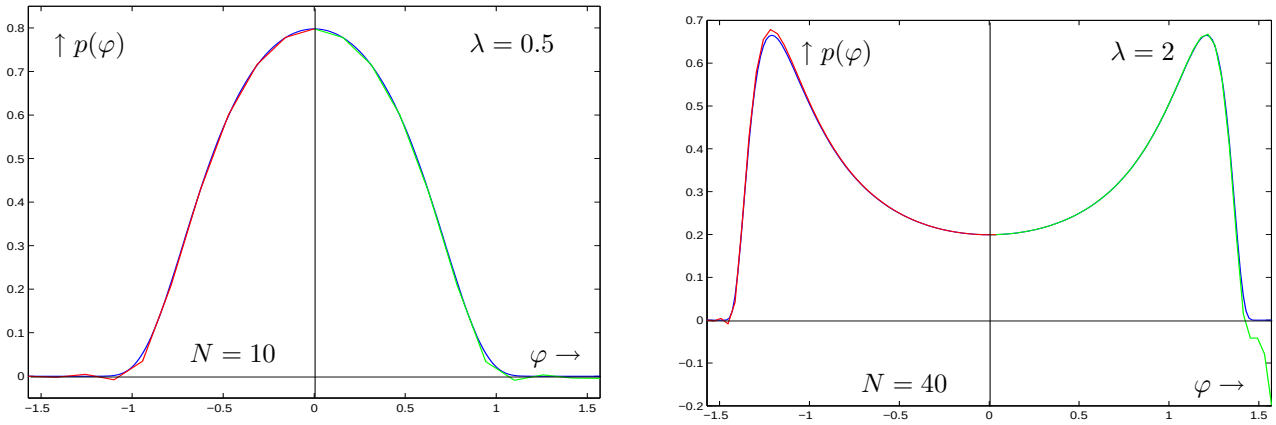

Fig. 3 Discrete and exact solutions of the second order Fokker-Planck equation (14) for $\lambda = 0.5$ and 2.0.

5 Large-scale quadratic optimization programming.

For further improvements higher order schemes may be applied or more efficiently large-scaled quadratic optimization to avoid negative results in the density tales. For these purposes the scalar equations (15) are written into the vector form $Ap = b$.

$$\begin{bmatrix} \alpha_1 & \beta_1 & 0 & \ldots & 0 \\ \gamma_2 & \alpha_2 & \beta_2 & \ldots & 0 \\ \vdots & & & & \vdots \\ 0 & 0 & \ldots & \gamma_{N-1} & \alpha_{N-1} \end{bmatrix} \begin{bmatrix} p_1 \\ p_2 \\ \vdots \\ p_{N-1} \end{bmatrix} = \begin{bmatrix} -\gamma_1 p_0 \\ 0 \\ \vdots \\ -\beta_{N-1} p_N \end{bmatrix}. \tag{18}$$

Solving this system under the boundary conditions $p_0 = 1$ and $p_N = 0$, the first N_{eq}-density values, obtained, are positive. Only in the tale range for $N_{eq} < n < N$, there are negative density values beginning with $p_{N_{eq}} < 0$. For the special example $N = 24$ and $\lambda = .5, 1, 2$ shown on the left side of figure 4, these numbers are $N_{eq} = 17, 20$ and 22. Naturally, negative density

values are physically meaningless and can only be explained by the approximating procedure in the tale range where density solutions strongly approach zero. To avoid these inconsistencies, it is proposed to apply large-scale quadratic programming, given e.g. in Matlab 6.1. Accordingly, the best approximation of the equation system $Ap = b$ under the constraint conditions

$$p \geq 0, \ (\text{N-1 lower bounds}), \qquad A_{eq}p = b_{eq}, \ (N_{eq} \text{ equality constraints}) \tag{19}$$

is calculated by minimizing the quadratic equation error

$$(Ap - b)^T(Ap - b) = \text{Min!}, \qquad \Rightarrow p^T A^T Ap - 2b^T Ap = Min! \tag{20}$$

Typical numerical results of this minimizing procedure are shown on the right-hand side of figure 4. Particularly for $\lambda = 2$ and $N = 24$ the optimization results are still good. In contrast to the classical results on the left side of figure 4 there are no negative density values on the right-hand side. Of course, the non-negative density values, obtained by the quadratic optimization, converge towards the exact solutions shown in figure 4 for increasing N and decreasing step size $\Delta\varphi$, respectively.

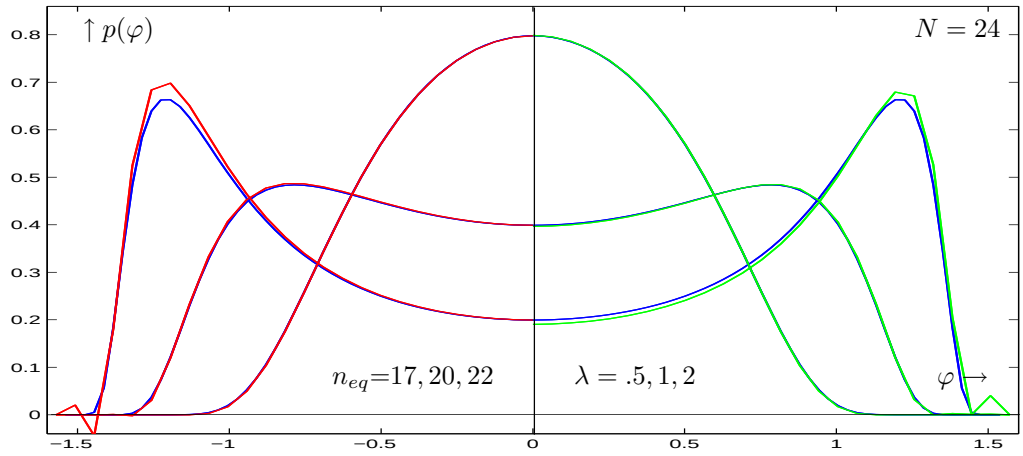

Fig. 4 Discrete, exact and optimized solutions of the Fokker-Planck equation (14).

6 Summary and concluding remarks.

To solve Fokker-Planck equations by central differences schemes with optimally selected boundary conditions, the infinite solution range is reduced to a finite one utilizing suitable mappings. The paper investigates large-scale quadratic programming to avoid negative probability densities in the tales. Further improvements can be achieved by higher order differences schemes or by adaptive finite elements.

References

[1] S. F. Wojtkiewicz, L. A. Bergman, E. A. Johnson, B. F. Spencer Jr., M. C. Grigoriu, Stochastic Response to Additive Gaussian and Poission White Noises, in: Stochastic Structural Dynamics, Spencer & Johnson (eds), Balkema, Rotterdam, 53-60, (1999).

[2] U. v. Wagner & W. V. Wedig. On the Calculation of Stationary Solutions of Multi-Dimensional Fokker-Planck Equations by Orthogonal Functions, in: Nonlinear Dynamics **21, 3** , 289-306, (2000).

[3] A. Naess & V. Moe, New Techniques for Path Integral Solution of the Random Vibration of Non-Linear Oscillators, in: Proceedings Icossar '97, Kyoto, Japan, Rotterdam, Balkema (1997).

[4] T. F. Coleman and Y. Li, A Reflective Newton Method for Minimizing a Quadratic Function Subject to Bounds on some of the Variables, Siam Journal on Optimization, **6, 4**, 1040-1058, (1996).

[5] L. Arnold, Random Dynamical Systems, (Berlin, Springer, 1998).